



Missouri University of Science and Technology
Scholars' Mine

International Specialty Conference on Cold-Formed Steel Structures

(1986) - 8th International Specialty Conference on Cold-Formed Steel Structures

Nov 11th, 12:00 AM

Flexural-torsional Buckling of Storage Rack Columns

O. Roos

Gregory J. Hancock

Follow this and additional works at: <https://scholarsmine.mst.edu/isccss>

 Part of the [Structural Engineering Commons](#)

Recommended Citation

Roos, O. and Hancock, Gregory J., "Flexural-torsional Buckling of Storage Rack Columns" (1986). *International Specialty Conference on Cold-Formed Steel Structures*. 3. <https://scholarsmine.mst.edu/isccss/8iccfss/8iccfss-session4/3>

This Article - Conference proceedings is brought to you for free and open access by Scholars' Mine. It has been accepted for inclusion in International Specialty Conference on Cold-Formed Steel Structures by an authorized administrator of Scholars' Mine. This work is protected by U. S. Copyright Law. Unauthorized use including reproduction for redistribution requires the permission of the copyright holder. For more information, please contact scholarsmine@mst.edu.

FLEXURAL-TORSIONAL BUCKLING OF STORAGE RACK COLUMNS

G. J. HANCOCK* and O. ROOS**

Summary

A theoretical and experimental study is presented of the flexural-torsional mode of buckling of the columns forming the upright frames of industrial steel storage racks. The particular frames studied were manufactured by bolting the bracing members to the column sections.

A comparison of the measured buckling modes is made with those predicted using a finite element buckling analysis based on one dimensional monosymmetric thin-walled elements. The theoretical buckling load is also derived using the Timoshenko formula for flexural-torsional buckling based on different effective lengths for flexure and torsion. This latter value is compared with the values computed using the finite element model.

The theoretical maximum loads, derived by substituting the theoretical elastic buckling loads and the experimental stub column strengths into the unfactored AISI column design curve, are compared with the test failure loads.

* Associate Professor, School of Civil and Mining Engineering,
University of Sydney, N.S.W., Australia, 2006

** Civil Engineer, Australian Atomic Energy Commission,
New Illawarra Rd., Menai, N.S.W., Australia, 2234

1. Introduction

A significant mode of buckling in the design of steel storage rack columns is the flexural-torsional mode, especially for channel section columns whose width and depth are approximately equal. For columns in braced frames, where the bracing is attached to the columns by bolting to additional flanges projecting from the channel lips, the channel section is usually wide and hence flexural-torsional buckling out of the plane of the frame normally occurs before flexural buckling in the plane of the upright. In addition, the nature of the bolted connection often results in flexibility of the connection which produces an increased torsional effective length and hence a lowering of the flexural-torsional buckling load.

This paper describes a series of tests on subassemblages consisting of steel storage rack columns braced into upright frames using bolted connections. The subassemblages were designed to have effective lengths for flexure and torsion which would be approximately equal to those in a prototype structure. The flexural and torsional deformations at points along the upright were measured in the tests to determine the mode of buckling and are described in the paper.

The test results are compared with a finite element buckling analysis (Refs. 2,5) based on thin-walled line elements of monosymmetric section. The effect of joint flexibility in the bolted connections between the uprights and the braces is demonstrated by comparison of the theoretical and experimental buckling modes.

In the RMI Specification for the Design of Steel Storage Racks (Ref. 8), recommendations are made for the selection of effective lengths in flexure and torsion for use in design. These effective lengths are then substituted in the Timoshenko formula for flexural-torsional buckling (Ref. 10) to determine the theoretical flexural-torsional buckling load for use in the unfactored column design curve given in the AISI Specification (Ref. 1). The test results are compared with design values produced using this procedure.

2. Choice of Test Configuration

2.1 Bracing in Prototype Structures

The usual configuration of a selective rack structure consists of a series of braced frames of one of the types shown in Fig. 1(a) connected together by a series of pallet beams as shown in Fig. 1(b). The connections between the pallet beams and the column sections of the upright frames are usually simple mechanical interlocks and so they are not fully rigid. Consequently, if the frames sway in the unbraced direction, these semi-rigid joints are required to assist in resisting the sway deformations.

The connections between the braces in the plane of the uprights and the column sections may be either welded or bolted, as shown in Fig. 2(a). In the case of the bolted system, it is possible to have both braces intersecting at a point in the column as shown in Figs. 1(a)(i) and 1(a)(ii). However, for welded systems, it is usual to have the points of

connection of adjacent braces separated, as shown in Figs. 1(a)(iii) and 1(a)(iv).

The torsional effective length, $K_T L_T$, defined in the RMI Specification for use in the design of columns, is based upon the unbraced length, L_T , shown in Fig. 1(a) and the effective length factor K_T . The effective length factor depends primarily upon the torsional rigidity of the connections between the columns and braces. For most bolted or welded connections, it is approximately equal to 1.0 provided a reasonable connection of the type shown in Fig. 2(a) is used.

The flexural effective length, $K_x L_x$, defined in the RMI Specification for flexural buckling of the columns perpendicular to the plane of the upright frames is based upon the pallet beam spacing L_c shown in Fig. 1(b) with $L_x = L_c$, as well as the effective length factor K_x . The effective length factor depends upon the flexural rigidities of the adjoining beams and columns, as well as the flexibility of the connection between the beams and columns. A method for assessing this latter flexibility is given in the RMI Specification using a portal sway test. For most practical frames, which are not braced against sidesway, K_x varies between 1.3 and 2.0. The value recommended in the RMI Specification, for frames where a rational analysis is not performed, is 1.7.

2.2 Test Configuration

The aim of the test programme was to design and test a subassemblage of upright frame which could be loaded in a compression testing machine such that the effective lengths for flexure and torsion would be similar to those described in 2.1 above. The testing configuration used is shown in Fig. 3. In the configuration shown, one column of the upright is tested in compression between spherical seats located on the line of the centroid of the full section and positioned on thick plates welded to the ends of the section as shown in Fig. 4(a). The second column is unloaded but prevented from moving perpendicular to the plane of the frame at the two points shown as R1 and R2 in Fig. 3. Consequently the loaded column is free to deform out of the plane of the frame but is partially prevented from twisting at the three points where the braces are connected to the column.

The effective length for flexure of the column perpendicular to the frame is equal to the distance between the spherical seats of 2590 mm (102 in). This length is equal to approximately 1.7 times 1524 mm (60 in) which is a practical beam spacing L_c . The distance between the brace locations is 1200 mm (47.2 in) which combined with a torsional effective length factor, K_T , of 1.0 gives a torsional effective length of 1200 mm (47.2 in). This value is considerably less than the flexural effective length but is in keeping with practical applications.

The cold-formed section used in the tests was described in detail in an earlier paper (Ref. 6) where its distortional buckling mode was investigated in detail. The geometry of the test section is shown in Fig. 2(b) and its dimensions are given in Table 1. The slots in the front face, which are normally used for connection of pallet beams, were not included in this test series. However the slots in the rear flanges, which are necessary to bolt the braces to the columns, were included. The section properties were computed using program OPEN (Ref. 7) and are given in

Table 2. The computed section properties do not include the slots in the rear flanges but do include the corner radii which were approximated by two straight chordal elements.

The braces were bolted between the rear flanges as shown in Fig. 2(a) with one brace inclined upwards and one downwards at each point as shown in Fig. 4(b). The braces were assumed to be unstressed in the test configuration in Fig. 3. The brace dimensions are given in Table 1 and its section properties in Table 2.

2.3 Instrumentation

One of the main objectives of the test programme was to compare the measured flexural-torsional buckling modes with those computed theoretically using a finite element analysis. Hence it was necessary to determine the lateral deflection and twist rotation at several points along the loaded columns. Three dial gauges, as shown in Fig. 3(b), were located at each of the five stations shown in Fig. 3(a). The twist rotation and lateral deflection of the web could be easily determined from these three gauges. A photograph of the gauges is shown in Fig. 4(a).

3 Test Results

3.1 Tests Performed and Loading

Two nominally identical upright columns were tested to destruction in an Amsler 500 tonne compression testing machine. The same unloaded column and braces were used for each test. The only significant difference between the test configurations was the tightness of the bolted connection at the central brace point of the loaded column. During the early stages of loading of the second frame, an opening was observed between the rear flange of the loaded column and brace at the central connection. This opening could only be attributed to a lack of proper tightening of the bolt in the joint. Column 1 was loaded in 5.0 kN (1.12 kip) increments up to a failure load of 87.5 kN (19.7 kip). Column 2 was loaded in 10.0 kN (2.25 kip) increments up to 60.0 kN (13.5 kip) then in 5.0 kN (1.12 kip) increments to failure at 77.5 kN (17.4 kip).

3.2 Test Deflections and Rotations

The lateral deflections of the web at the central dial gauge location are shown in Fig. 5(a). Test 2 deflected considerably more than test 1 at loads above 25kN (5 kips approx.). The deformation modes measured along the loaded columns are shown in Fig. 6 for both tests at loads near the ultimate load. The positive sign convention for deflections and rotations is shown in Fig. 5(b).

As shown in Fig. 5(b)I, the rotation at the central dial gauge location would be positive if the column section and braces were rigidly connected. However, as shown in Fig. 6, the rotation at the central dial gauge location had a negative sign. This negative rotation could only occur simultaneously with a positive deflection if the section or connection deformed as shown in Fig. 5(b)II.

The rotational deformations of Test 1 shown in Fig. 6 demonstrate considerably more restraint to negative torsional deformations than for Test 2. Hence it appears that the connection between the braces and column are very important in resisting torsional deformation of the column. It has also been concluded that the bolted connection at the central brace point in Test 2 must have been considerably looser than in Test 1.

3.3 Joint Torsional Flexibility Test

A small test apparatus was designed and used to determine the torsional flexibility of the brace to column joint. A plan view of the test is shown in Fig. 7(a) and an end elevation in Fig. 7(b). The column end supports were designed to allow longitudinal warping displacements but to prevent lateral displacement and torsional rotation. This was achieved by holding the channel sections by a pair of pins located through holes adjacent to the ends of the channel at the two points of zero sectorial co-ordinate (zero warping displacement) in the cross-section. The bracing members were attached to the column section in exactly the same manner as in the sub-assembly tests except that the braces were both perpendicular to the longitudinal axis of the channel. The final tightening of the column bracing connection bolt was achieved using a torque-wrench to a torque of 6.8 Nm (5.0 lb.ft)

The assembly was loaded perpendicular to its plane as shown in Fig. 7(b) using 22.2 N (5.0 lb) increments to 156.7 N (35.0 lb). The resulting load deflection graph is shown in Fig. 7(c). The process was repeated with the bolted connection slackened by one half a turn. The results of this test are also given in Fig. 7(c). It is interesting to note the stiffening of the slackened joint for loads above 66.7 N (15 lb). The incremental (tangent) stiffness of the slackened joint approaches that of the torqued joint as the load is increased.

The deflection resulting from the joint flexibility was determined by subtracting the deflection components resulting from:

- (a) Cantilever deflection of bracing
- (b) Bending deflection of the column
- (c) Deflection due to twisting of the column

The resulting joint flexibility can be expressed as a relation between applied torque and rotational deformation of the joint.

For the torqued joint, the resulting joint flexibility was computed to be 0.153 radians/kN.m (0.0173 radians/kip.in). The joint flexibility of the slackened joint is a secant value which varies with the load on the joint. The secant value at a load of 66.7 N (15 lb) was 0.476 radians/kN.m (0.0549 radians/kip.in). As demonstrated later, these values can be incorporated into the finite element buckling analysis.

4 Computer and Theoretical Models

4.1 Finite Element Model

4.1.1 Thin-Walled Element

The thin-walled members forming the upright frames have been modelled using the thin-walled line element shown in Fig. 8. This element, which is the same as that used in Refs. 2,5, is replaced by a line on the shear centre axis with four nodal displacements representing out of plane displacements at each end. As shown in Fig. 8, these displacements are:

- (a) The displacement of the shear centre perpendicular to the plane of symmetry (u_1)
- (b) The rotation of the shear centre axis about the symmetry axis (u_1')
- (c) The twist rotation (ϕ_1)
- (d) The rate of change of twist rotation (ϕ_1') which represents the warping displacement at the node.

The strain energy (U) of a thin-walled element and the potential energy (V) of a concentric axial force (P) can be computed using the expressions given in Appendix 1. The second term in the potential energy expression, which involves the shear centre co-ordinate y_0 , was not included in Refs. 2,5 but has been included in this study (Ref. 4).

The lateral deflection, u , of the shear centre axis and the torsional rotation, ϕ , have each been represented by a cubic polynomial whose coefficients are based on the nodal displacements shown in Fig. 8.

The stiffness [k] and stability [g] matrices for the thin-walled element were determined using conventional procedures based on application of the principle of minimum total potential energy taken with respect to the out of plane buckling deformations (Ref. 5).

4.1.2 Frame Model

The line element model of the frame is shown in Fig. 9 with the loaded column subdivided into 6 elements as shown. The line elements shown represent the shear centre axes of the members. The small elements numbered 2-8, 4-9, 6-10, 11-15, 12-16, 13-17 and 14-18 represent a link between the line of the shear centre axis and the bolt location in the column-brace joint. The out of plane bending flexibility of these link elements has been selected to represent the torsional flexibility of the joints as determined in Section 3.3 above.

The global stiffness [K] and stability [G] matrices were assembled from the element stiffness and stability matrices taking account of the relative orientation of the elements at a node. The warping displacements, represented by the degree of freedom (ϕ_1) at each node, have been taken as continuous along the loaded and unloaded columns. The warping restraint, which would come from the link elements connected to the columns if warping compatibility was assumed between the column elements and the link elements, has been eliminated from the global stiffness and stability matrices by

modification of the warping stiffnesses of the link elements. This procedure, which is equivalent to putting a flexural pin in the end of a flexural member to eliminate flexural compatibility, has been called "insertion of a warping pin". A detailed description and verification of this process is given in Ref. 9.

The global constraints applied to the resulting global stiffness and stability matrices consist of:

- (a) prevention of lateral displacements at nodes 16, 17 as a result of restraints R1 and R2 in Fig. 3(a).
- (b) prevention of warping displacements at nodes 1, 7 as a result of the plate welded to the ends of the loaded column.
- (c) prevention of lateral displacements at a point on the line of the centroid of the section at nodes 1, 7 as shown in Fig. 9.

The eccentricity of the restraint at nodes 1 and 7 results from the fact that the ball joint at the ends of the column, as shown in Fig. 4(a), is located on the line of the section centroid to ensure concentric loading. The eccentric restraint is accounted for by taking the appropriate linear combinations of the lateral displacements (u_i) and torsional rotations (ϕ_i) at nodes 1 and 7, so as to represent the lateral displacement at the centroid, and then equating these lateral displacements to zero. The detailed verification of this process is given in Ref. 9.

4.1.3 Buckling Loads and Modes

The resulting eigenvalue problem was solved using the direct eigenvalue routines of the type described in Ref. 3 to determine the buckling loads and modes. The analysis was performed three times as set out in Table 3. The first analysis (F.E. 1), which did not include the effects of warping pins, eccentric restraints at nodes 1 and 7, and any joint flexibility produced a buckling load of 128.7 kN (29.0 kips), as given in Table 3, and the buckling mode shown in Fig. 10(a). It is interesting to observe that the analysis with the rigid connection between the brace and column produces a positive rotation at the centre of the column of the type shown in Fig. 5(b)I.

The specific features, which were incorporated in the original analysis so that it would accurately model the test frames, were then included in the second (F.E. 2) and third (F.E. 3) analyses as set out in Table 3. These features were the warping pins in the link elements as described above, the eccentric restraints at Nodes 1 and 7 as described above and the flexible column-brace connections. The joint flexibilities for the second and third analyses were based on the values determined in Section 3.3 for the tight joint and the slackened joint respectively. The latter value was based on the secant value of the joint flexibility of the slackened joint as it began to stiffen under deformation.

The second analysis (F.E. 2), which assumed that the brace-column joint was tight, produced a critical load of 104.5 kN (23.5 kips) with the buckling mode shown by the solid line in Fig. 10(b). The rotation at the centre of the column has a negative sign, as observed in the tests. The third analysis (F.E. 3), which assumed that the brace-column joint was slackened,

produced a critical load of 93.3 kN (21.0 kips) with the buckling mode shown by the dashed line in Fig. 10(b). The negative rotation at the brace-column joint has a larger magnitude for the slackened joint than for the tight joint. The theoretical buckling modes have an arbitrary magnitude. However, they have been adjusted to give comparable values with the test results in Fig. 6.

4.2 Timoshenko Formula

The Timoshenko formula for flexural-torsional buckling perpendicular to the plane of symmetry (Ref. 10) is based on the Euler flexural buckling load (P_{Oy}) and the torsional buckling load (P_{Oz}), as set out in Appendix II. The RMI Specification (Ref. 8) allows the effective length for flexure, to be used in computing P_{Oy} , to be different from the effective length in torsion to be used in computing P_{Oz} . This difference is not correct theoretically, since the flexural and torsional components of the buckle are assumed in the theoretical derivation to be the same half-wavelength. However, the assumption appears acceptable empirically, and has been used in this paper for comparison of the Timoshenko formula with the finite element analyses.

As given in Table 3, the value computed using the Timoshenko formula with $K_y L_y = 2590$ mm (102 in) and $K_T L_T = 1200$ mm (47.2 in) is 75.5 kN (17.0 kips). Note that the y-axis has been taken in the plane of symmetry in the theoretical calculations in this paper.

5 Column Strength

In order to compare the theoretical models with the test column strengths, it is first necessary to compute the theoretical maximum column strengths from the theoretical buckling loads. The approach adopted in this paper was to use the column design curve in the AISI Specification (Ref. 1) with the factor of safety of 1.92 eliminated from the denominator. The resulting formula is:

$$P_{\max} = QP_y - (QP_y)^2 / 4P_{Oc}$$

where P_{\max} = the theoretical maximum column strength

QP_y = the stub column strength

P_{Oc} = the theoretical elastic buckling load

The stub column strength was determined experimentally to be 127 kN (28.6 kips) for the column section. The resulting theoretical maximum column strengths are given in Table 4 where they are compared with the frame test strengths.

The finite element model 1, which assumed the brace-column joint to be rigid, significantly overestimates (95.7 kN) the test column strengths (87.5, 77.5 kN). The finite element model 2, which assumed a tight but flexible joint, provides an accurate estimate (88.4 kN) of Test 1 (87.5 kN). The finite element model 3, which assumed a slackened joint, provides a slightly unconservative estimate (83.8 kN) of Test 2 (77.5 kN). This latter variation is to be expected since the tightness or otherwise of the

the central brace-column connection in Test 2 was not quantified. The strength computed using the Timoshenko formula for flexural-torsional buckling (73.6 kN) produces a conservative but reasonable estimate of the column strengths (87.5, 77.5 kN).

6 Conclusions

A pair of tests on subassemblages of upright frames of steel storage racks, manufactured by bolting the columns and braces together, has been described in detail. These tests were designed to produce effective lengths in flexure and torsion which would be similar to those in full scale frames. The flexural-torsional deformation modes of the test frames were carefully measured, as were their maximum load capacities.

A finite element model for planar frames composed of monosymmetric thin-walled elements was proposed. The theoretical buckling modes computed using the finite element model were compared with those measured in the tests. The flexibility of the brace-column connection was found to have a very significant effect on the buckling loads and modes computed. The deformation modes of the test frames were found to be similar to the buckling modes computed assuming flexible joints.

The maximum strength model based on the finite element analysis, in which a tight but flexible joint was assumed, accurately predicted the strength of Test 1. The maximum strength model based on the finite element analysis in which a slackened joint was assumed, was found to be very sensitive to the joint flexibility. The maximum strength model based on the Timoshenko formula for flexural-torsional buckling with K_T equal to 1.0 was found to produce conservative estimates of the test strengths.

The bolted connections between columns and braces in steel storage rack systems manufactured by bolting, rather than by welding, should be fully tightened to ensure adequate strength.

7 References

1. American Iron and Steel Institute, Specification for the Design of Cold-Formed Steel Structural Members, Washington, DC (1983).
2. Barsoum, R.S., and Gallagher, R.H., Finite Element Analysis of Torsional and Flexural-Torsional Stability Problems, International Journal for Numerical Methods in Engineering, Vol. 2, 1970, p. 335.
3. Bishop, R., Gladwell, G. and Michaelson, S., The Matrix Analysis of Vibration, Cambridge University Press, 1965.
4. Bleich, F., Buckling Strength of Metal Structures, McGraw-Hill Book Co., Inc., New York, N.Y., 1952
5. Hancock, G.J. and Trahair, N.S., Finite Element Analysis of the Lateral Buckling of Continuously Restrained Beam-Columns, Civil Engineering Transactions, Institution of Engineers, Australia, Vol. CE 20, No. 2, 1978.

6. Hancock, G.J., Distortional Buckling of Steel Storage Rack Columns, Journal of Structural Engineering, American Society of Civil Engineers, Vol. 111, No. 12, Dec. 1985.
7. Hancock, G.J. and Harrison, H.B., A General Method of Analysis of Stresses in Thin-Walled Sections with Open and Closed Parts, Civil Engineering Transactions, Institution of Engineers, Australia, CE14, No. 2, 1972.
8. Rack Manufacturers Institute, Specification for the Design, Testing and Utilisation of Industrial Steel Storage Racks, Chicago , 1979.
9. Roos, O., Flexural-Torsional Buckling of Steel Storage Rack Columns, M. Eng. Sc. Thesis, University of Sydney, 1985.
10. Timoshenko, S.P. and Gere, J.M., Theory of Elastic Stability, McGraw-Hill Book Co., Inc., New York, 1961.

8. Appendices

I Energy Terms for a Thin-Walled Element

$$U = \frac{1}{2} \int_0^L (EI_y)(u'')^2 dz + \frac{1}{2} \int_0^L (GJ)(\phi')^2 dz + \frac{1}{2} \int_0^L (EI_w)(\phi'')^2 dz$$

where U is the strain energy in the element

L is the length of the element

E is the Young's modulus

I_y is the second moment of area about the axis of symmetry

u is the displacement of the shear centre perpendicular to the plane of symmetry

G is the shear modulus

J is the torsion constant

I_w is the section warping constant

ϕ is the torsional rotation about the shear centre

' = d/dz

'' = d^2/dz^2

$$V = \frac{1}{2} \int_0^L P(u')^2 dz + \frac{1}{2} \int_0^L P(2y_0 u' \phi') dz + \frac{1}{2} \int_0^L P(r_1)^2 (\phi')^2 dz$$

where V is the potential energy of the concentric axial force (P) in the element

y_0 is the y co-ordinate of the shear centre

$(r_1)^2 = (I_x + I_y)/A + (y_0)^2$

II Timoshenko Flexural-Torsional Buckling Formula

$$P_{oyz} = \frac{(P_{oy} + P_{oz})^2 \pm \sqrt{\{(P_{oy} - P_{oz})^2 + 4P_{oy}P_{oz}(y_0/r_1)^2\}}}{2[1 - (y_0/r_1)^2]}$$

where P_{oyz} = flexural-torsional buckling load

$P_{oy} = \pi^2 EI_y / (K_y L_y)^2$

$P_{oz} = GJ \{1 + \pi^2 EI_w / GJ (K_T L_T)^2\} / (r_1)^2$

SECTION	A mm (in.)	B mm (in.)	C mm (in.)	D mm (in.)	E mm (in.)	F mm (in.)	S mm (in.)	t mm (in.)
COLUMN	13.7 (0.15)	90.1 (3.55)	38.0 (1.49)	9.6 (0.38)	7.0 (0.28)	32.0 (1.26)	10.0 (0.39)	1.66 (0.065)
BRACE	8.5 (0.33)	45.9 (1.81)	25.8 (1.01)	-	-	-	-	1.63 (0.064)

TABLE 1 MEAN MEASURED SECTION DIMENSIONS

SECTION	A mm ²	\bar{y} mm	I_x mm ⁴ x10 ⁶	I_y mm ⁴ x10 ⁶	J mm ⁴ x10 ⁶	y_o mm	I_w mm ⁴ x10 ⁹
COLUMN	394	-23.4	0.184	0.418	336	-50.8	0.434
BRACE	173	- 8.8	0.058	0.016	147	-21.5	0.008

$$1 \text{ in}^2 = 645 \text{ mm}^2$$

$$1 \text{ in}^4 = 41623 \text{ mm}^4$$

$$1 \text{ in}^6 = 268.5 \times 10^6 \text{ mm}^6$$

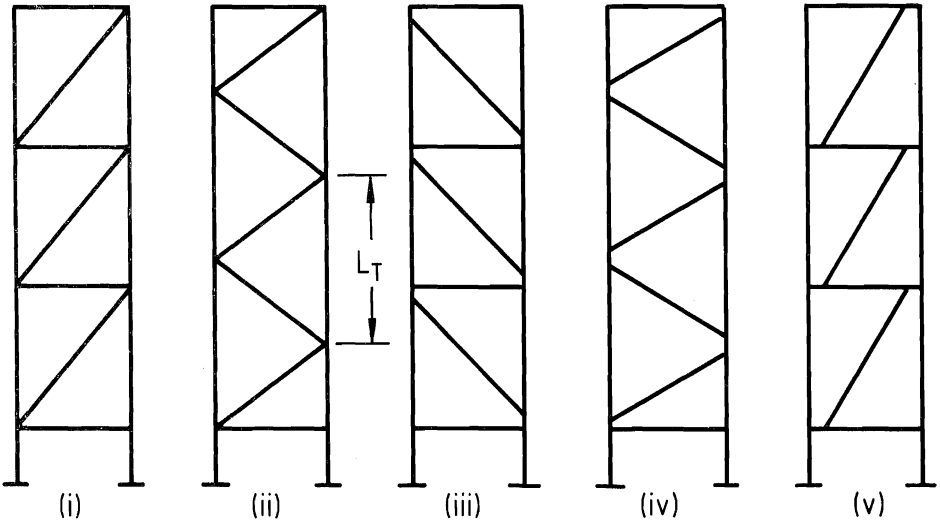
TABLE 2 COMPUTED SECTION PROPERTIES

MODEL TYPE AND NO.	JOINT TYPE	WARPING PINS IN LINKS	ECCENTRIC RESTRAINTS NODES 1,7	EFFECTIVE LENGTHS		BUCKLING LOAD kN (kips)
				$K_y L_y$ mm (in.)	$K_T L_T$ mm (in.)	
FINITE ELEMENT 1	RIGID	NO	NO	-	-	128.7 (29.0)
FINITE ELEMENT 2	TIGHT	YES	YES	-	-	104.5 (23.5)
FINITE ELEMENT 3	SLACK	YES	YES	-	-	93.3 (21.0)
TIMOSHENKO FORMULA	-	-	-	2590 (102)	1200 (47.2)	75.5 (17.0)

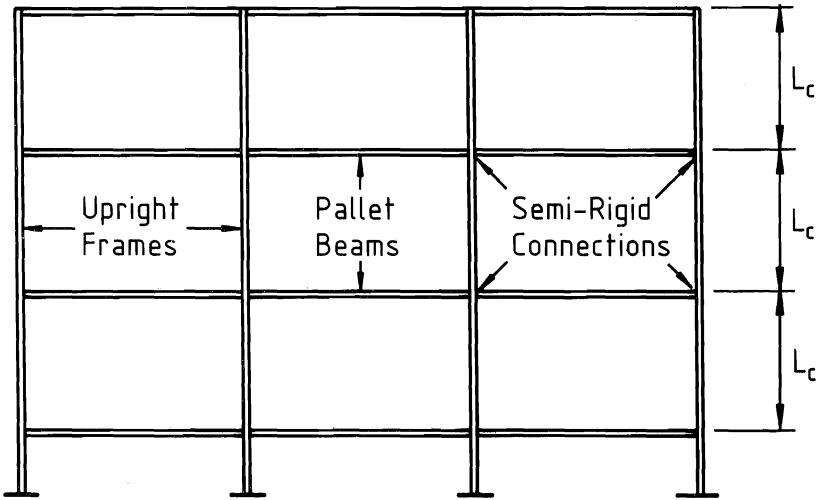
TABLE 3 THEORETICAL BUCKLING LOADS

MODEL/TEST NO.	STUB COLUMN STRENGTH kN (kips)	THEORETICAL BUCKLING LOAD kN (kips)	MAXIMUM LOAD kN (kips)
FINITE ELEMENT 1	127 (28.6)	128.7 (29.0)	95.7 (21.5)
FINITE ELEMENT 2	127 (28.6)	104.5 (23.5)	88.4 (19.9)
FINITE ELEMENT 3	127 (28.6)	93.3 (21.0)	83.8 (18.9)
TIMOSHENKO FORMULA	127 (28.6)	75.5 (17.0)	73.6 (16.6)
TEST 1	-	-	87.5 (19.7)
TEST 2	-	-	77.5 (17.4)

TABLE 4 MAXIMUM LOADS

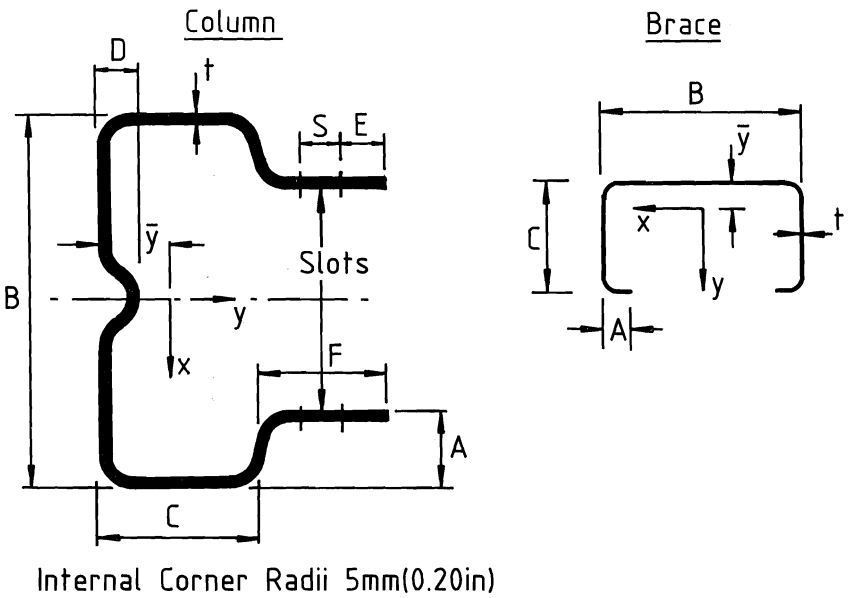
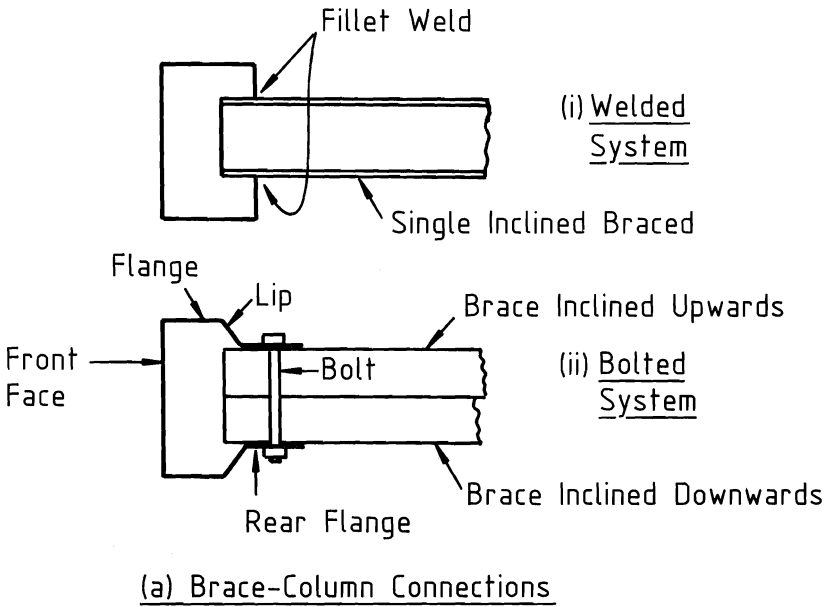


(a) Bracing in Plane of Upright Frames



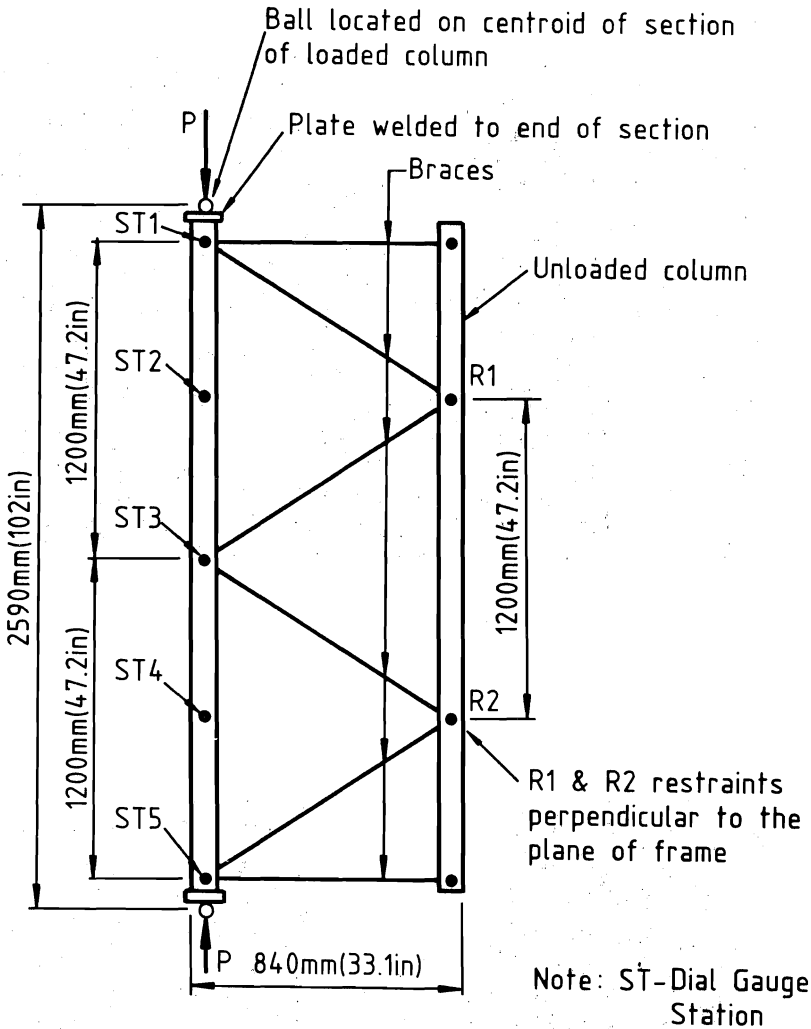
(b) Unbraced Plane

FIG.1 BRACING SYSTEMS

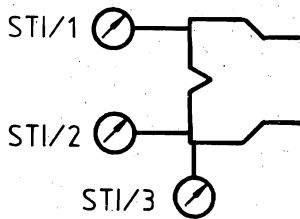


(b) Test Section Geometry

FIG.2 FRAME SECTIONS

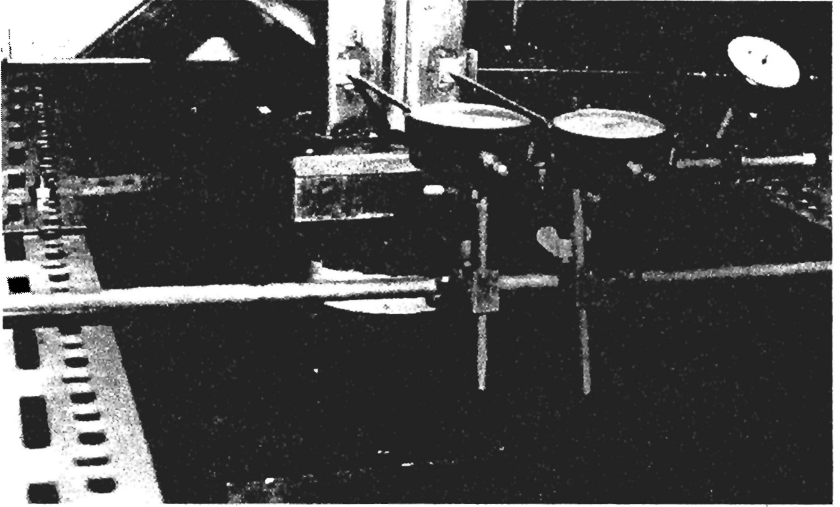


(a) Elevation

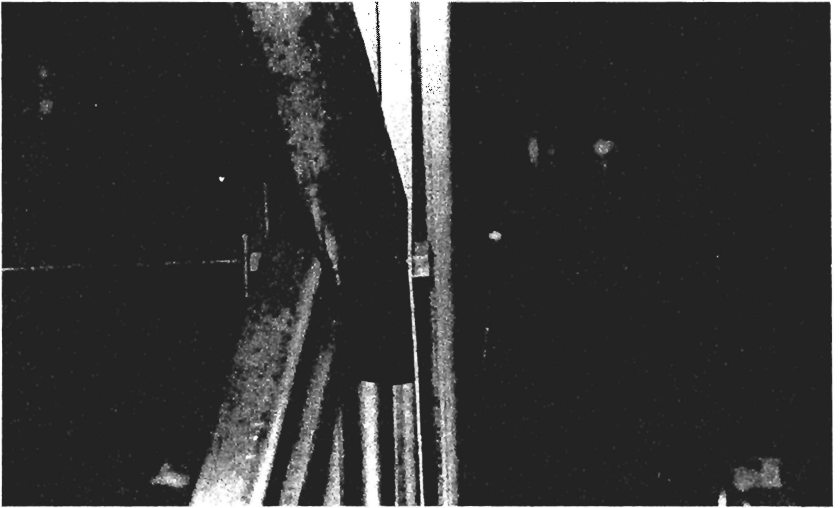


(b) Dial Gauge Locations

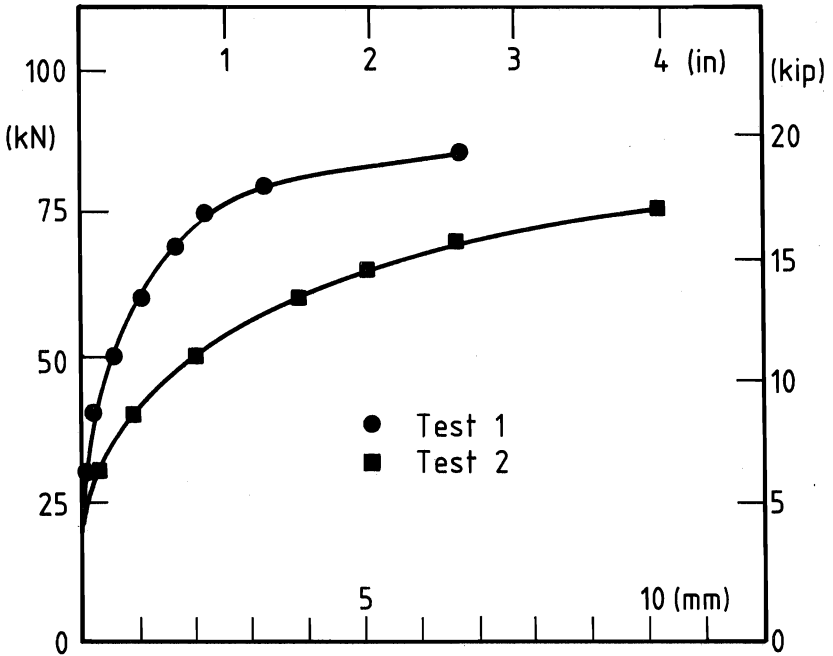
FIG.3 UPRIGHT TEST CONFIGURATION



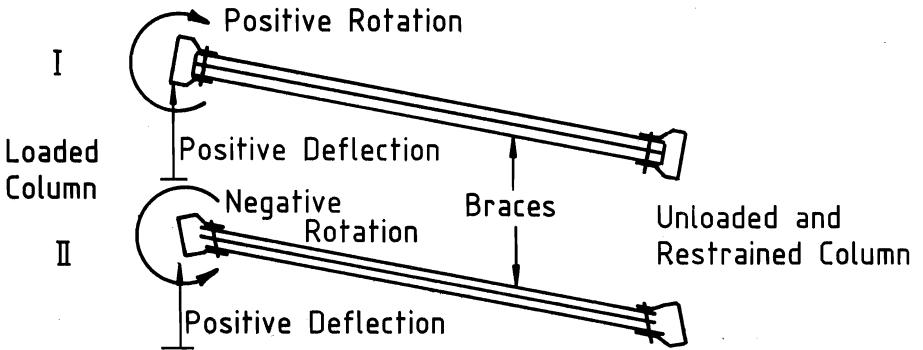
(a) Loading Point and Dial Gauges



(b) Bracing



(a) Lateral Deflections of Web



(b) Deflections and Rotations of Loaded Column

FIG.5 LATERAL DEFLECTIONS AT CENTRE OF LOADED COLUMN (ST3)

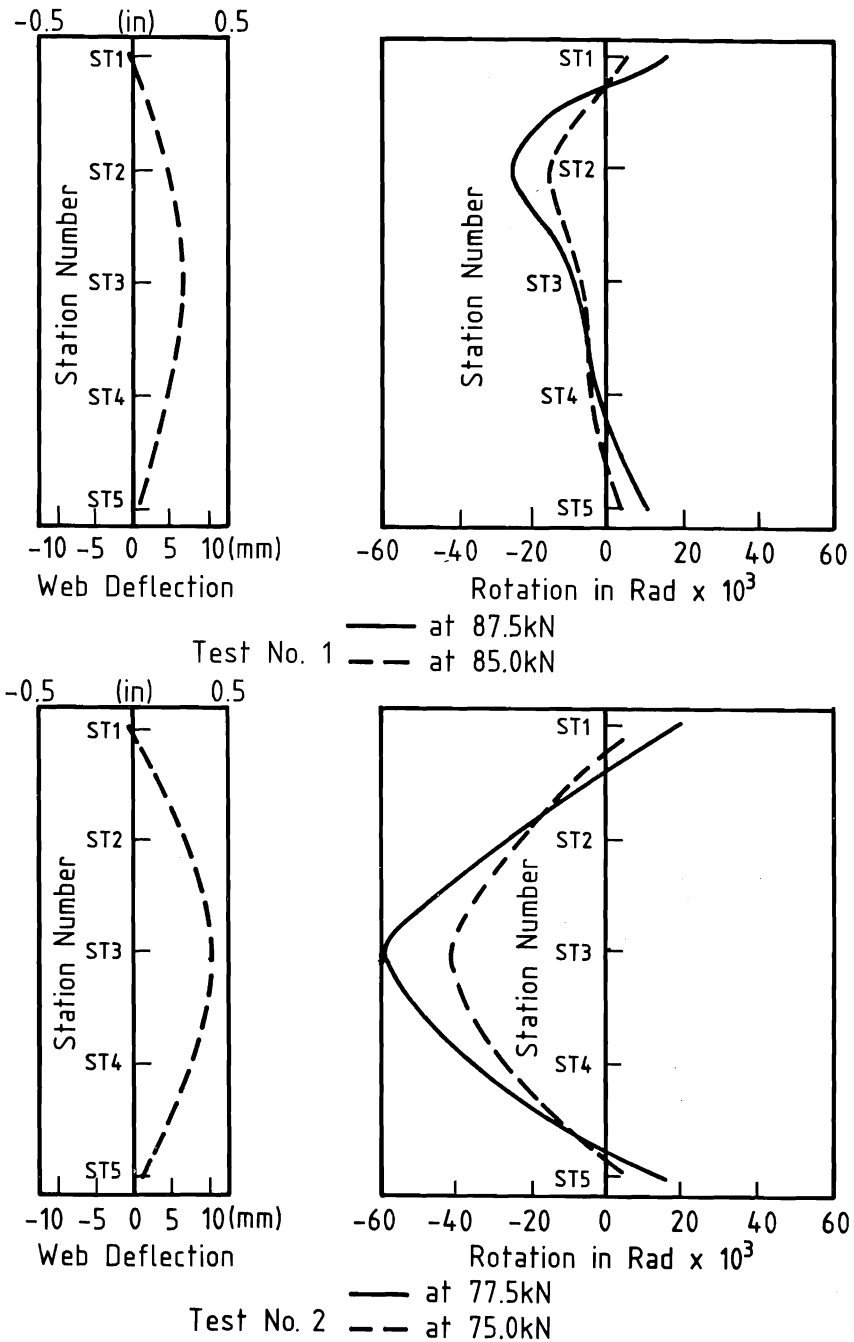
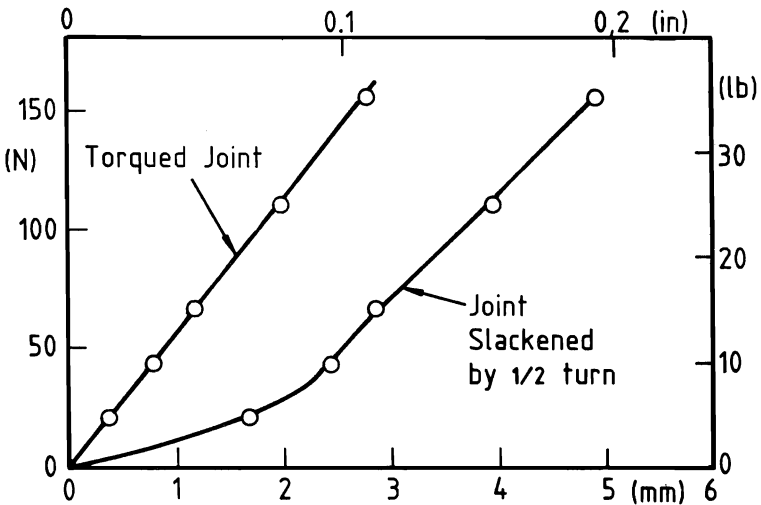
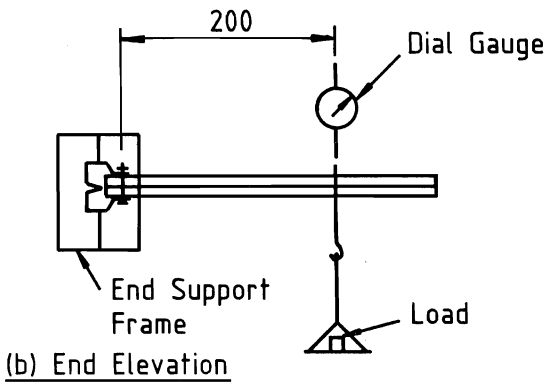
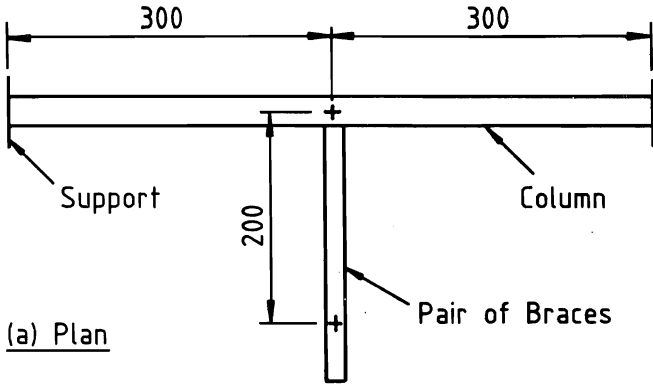


FIG.6 EXPERIMENTAL DEFORMATION MODES



(c) Load-Deflection Graph

FIG.7 JOINT TORSIONAL FLEXIBILITY TEST

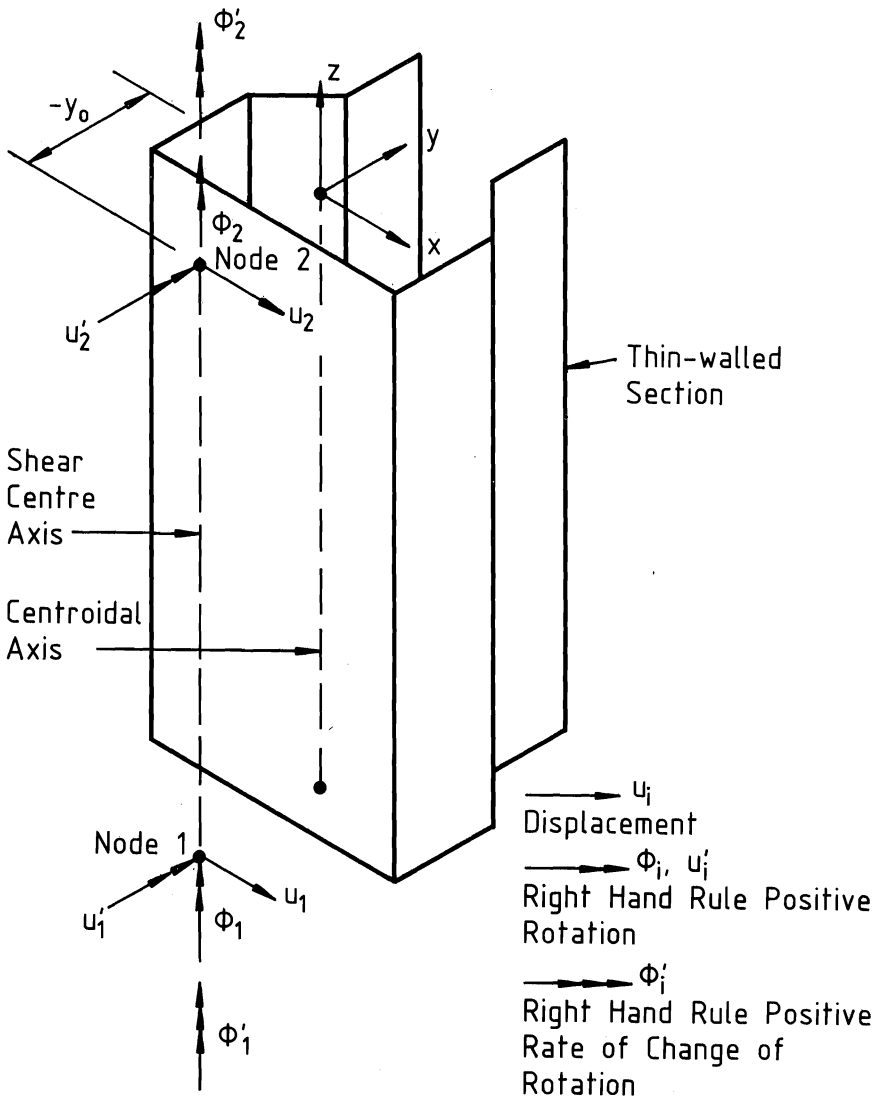
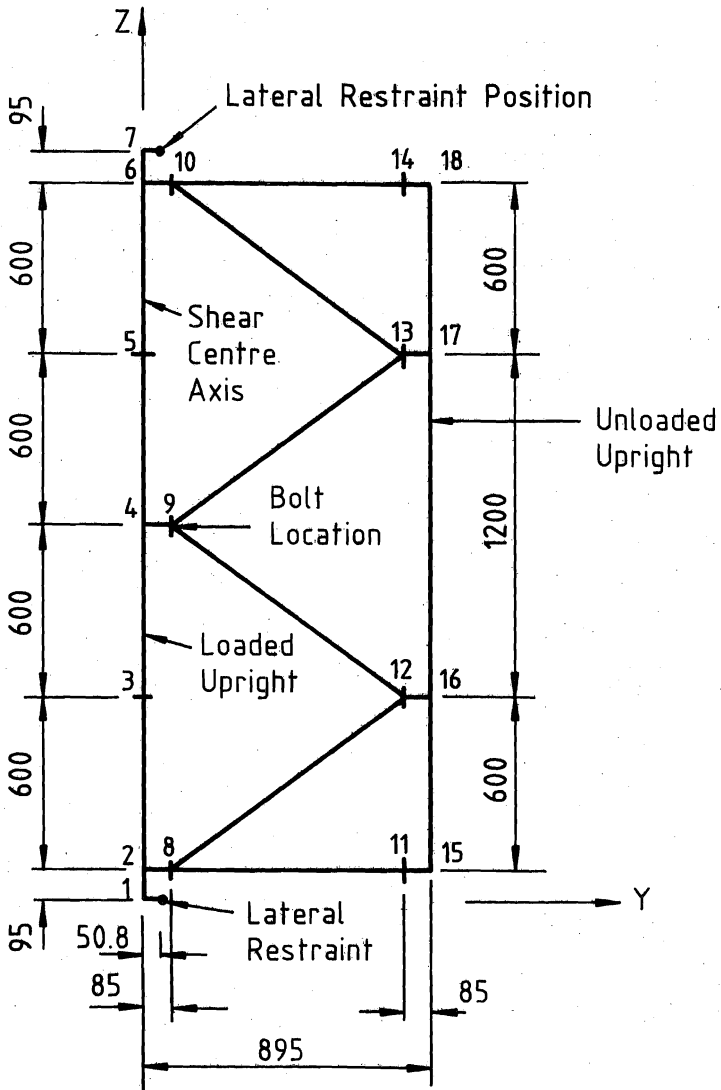
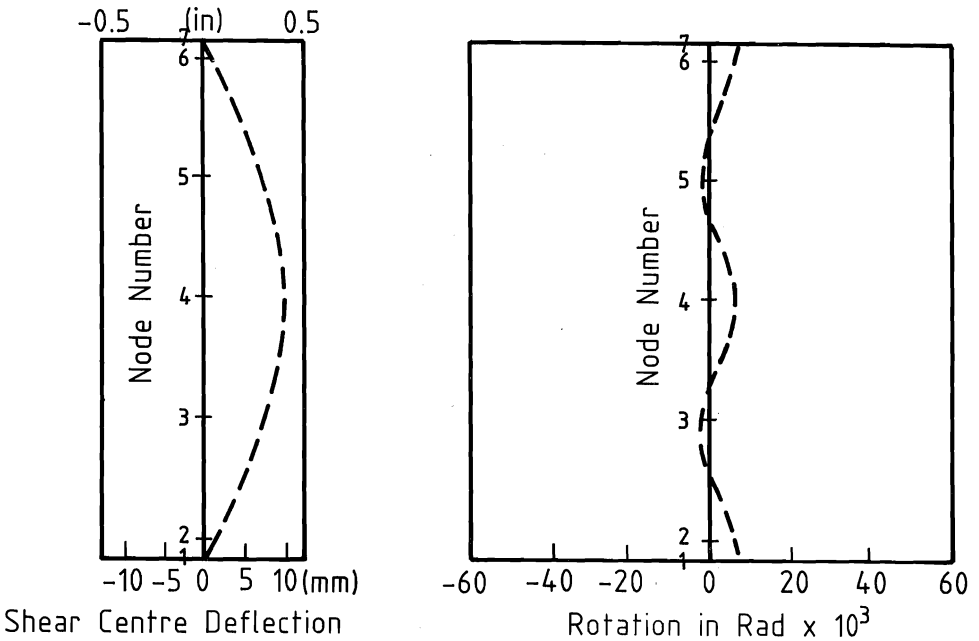


FIG.8 THIN-WALLED LINE ELEMENT

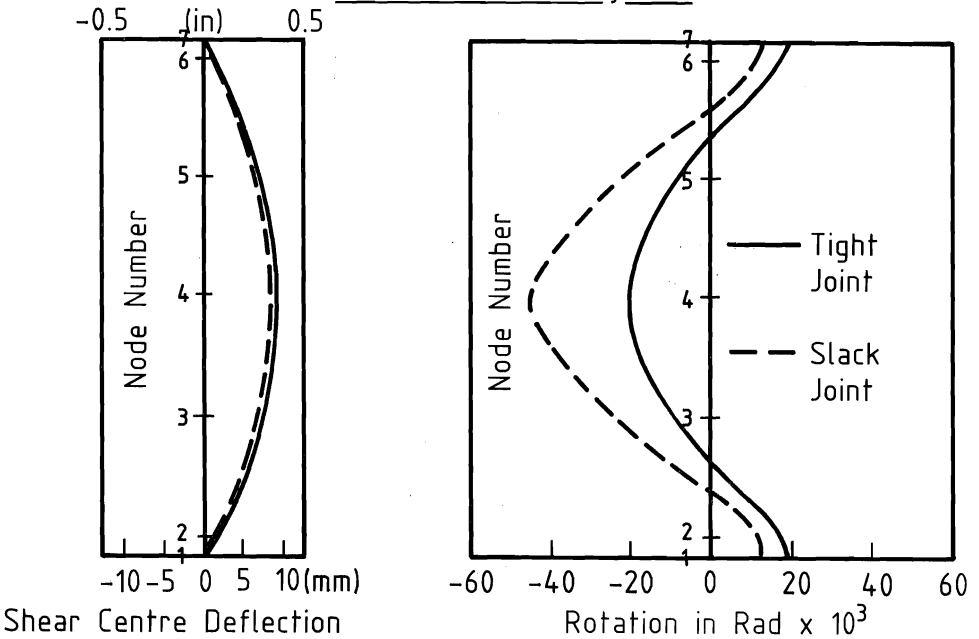


All dimensions in mm (1in.=25.4mm)

FIG.9 COMPUTER MODEL OF SUB-ASSEMBLAGE



(a) Finite Element Analysis 1



(b) Finite Element Analysis 2 and 3

FIG.10 THEORETICAL BUCKLING MODES